J. Shanghai Jiao Tong Univ. (Sci.), 2024, 29(4): 689-701
https://doi.org/10.1007/s12204-024-2728-x

Time-Varying Formation-Containment Tracking Control for Unmanned Aerial Vehicle Swarm Systems with Switching Topologies and a Non-Cooperative Target

WU Xiaojing∗ (武晓晶), *CAO Tongyao* (曹童瑶), *ZHEN Ran* (甄 然), *LI Zhijie* (李志杰)
(School of Electrical Engineering, Hebei University of Science and Technology, Shijiazhuang 050018, China)

Abstract: This paper studies the time-varying formation-containment tracking control problems for unmanned aerial vehicle (UAV) swarm systems with switching topologies and a non-cooperative target, where the UAV swarm systems consist of one tracking-leader, several formation-leaders, and followers. The formation-leaders are required to accomplish a predefined time-varying formation and track the desired trajectory of the tracking-leader, and the states of the followers should converge to the convex hull spanned by those of the formation-leaders. First, a formation-containment tracking protocol is proposed with the neighboring relative information, and the feasibility condition for formation-containment tracking and the algebraic Riccati equation are given. Then, the stability of the control system with the designed control protocol is proved by constructing a reasonable Lyapunov function. Finally, the simulation examples are applied to verify the effectiveness of the theoretical results. The simulation results show that both the formation tracking error and the containment error are convergent, so the system can complete the formation containment tracking control well. In the actual battlefield, combat UAVs need to chase and attack hostile UAVs, but sometimes when multiple UAVs work together for military interception, formation-containment tracking control will occur.
Keywords: formation-containment tracking control, switching topology, unmanned aerial vehicle (UAV)
CLC number: TP273 **Document code:** A

0 Introduction

Cooperative control of unmanned aerial vehicle (UAV) swarm systems has been attracted attention because it can be widely used in many fields, such as surveillance[1], source seeking[2], drag reduction[3], load transportation[4], and collaborative localization[5]. One of the most important research topics in cooperative control of multi-UAV systems is formation control, which requires all UAVs to accomplish the desired time-varying formation. There are many classical control strategies that can be used to solve the formation control problem of UAV swarm systems, including leader-follower[6], virtual structure[7], artificial potential energy[8], and behavior-based strategy[9]. In recent years, consensus approaches have been widely applied to study the formation control problems with the development of consensus control theory[10]. How to design a distributed controller with neighboring information to solve the formation control problem is a hot issue in current research.

Based on consensus control strategies, a completely distributed formation control protocol has been designed to solve the formation control problem of vertical take-off and landing (VTOL) UAVs with communication delays in Ref. [11]. Reference [12] has studied distributed finite-time formation control problems for multiple UAVs helicopter system with disturbances using consensus-based protocols. Based on the consensus strategy, a formation stabilization control problem for second-order multi-agent systems with actuator faults and directed topologies has been investigated in Ref. [13]. Reference [14] has proposed the consensus control protocols for the hybrid multi-agent systems to address the problem of formation control by using the matrix theory. Reference [15] has designed a distributed predictive formation controller of networked mobile robots with communication delay.

Besides formation control[16], another hot research topic in cooperative control of UAV swarm systems is containment[17], which is that the states of followers are required to converge to the convex hull spanned by the formation-leaders. Reference [18] has presented

Received: 2023-05-26 **Accepted:** 2023-09-05
Foundation item: the National Natural Science Foundation of China (No. 62003129)
∗**E-mail:** wuxiaojing013@163.com

the sufficient conditions for second-order multi-agent systems with inherent nonlinear dynamics to achieve containment control. The event-triggered adaptive containment control for the second-order linear multi-agent systems with time-varying input delays has been studied in Ref. [19]. Reference [20] has discussed containment problems for high-order multi-agent swarm systems with directed interaction topologies. The containment control problem for multi-agent systems with multiple leaders which have non-zero control inputs and input saturation has been investigated in Ref. [21]. Reference [22] has presented the necessary and sufficient conditions for multi-UAV systems with multiple stationary leaders to achieve containment. However, the defect of not being able to control the whole macroscopic movement of the swarm system effectively has existed in the containment control[17-21].

Based on the formation control and the containment control, more and more researchers realize that a more significant problem is formation-containment control, where the leaders need to accomplish a desired formation, and the followers need to converge to the convex hull spanned by the leaders at the same time. Reference [23] has studied formation-containment control problems for multiple multirotor UAV systems with directed topologies. The formation-containment control of second-order nonlinear multi-agent systems with communication delays has been addressed in Ref. [24]. Reference [25] has discussed the formation-containment control problems for high-order linear time-invariant multi-agent systems. The formation containment control under sampling and time delays for multi-agent systems has been studied in Ref. [26]. Reference [27] has designed the control algorithm using output feedback control strategy and observer-based to address the time-varying output formation-containment problem of multi-agent systems.

However, in many practical applications, accomplishing the time-varying formation containment is only the first step to complete target transport work in a complex environment. The multi-UAV systems should also track the target's trajectory such that all the UAVs can reach the desired destination safely. Therefore, the problem of time-varying formation-containment tracking control of multi-UAV swarm systems has been studied in Refs. [28-35]. References [28-29] have investigated the distributed formation-containment tracking issue for heterogeneous linear multi-agent systems and autonomous underwater vehicles (AUVs) respectively, but the tracking-leader with control input was not considered. In fact, the tracking-leader with unknown control input can regulate the expected trajectory such that they can avoid obstacles effectively, so it is meaningful to study the problem of formation-containment tracking of multi-agent systems with a tracking-leader of unknown control input. To solve the aforementioned problem, the time-varying formation-containment tracking control with unknown control input has been developed in Refs. [30-34]. References [30-33] have designed a formation-containment tracking protocol using the neighboring relative information for general multi-agent systems with unknown control input. Reference [34] has solved the problem of the predefined-time time-varying formation-containment tracking for the multiple Euler-Lagrange systems, where the external disturbances are taken into consideration. Nevertheless, note that the switching topologies have not been discussed in the above-mentioned research results. In practice, the topology structure among UAVs may cause the failure of the communication link and the creation of a new communication link due to the limitation of the communication distance. Therefore, it is meaningful to investigate the formation-containment tracking problems for multi-UAV systems with a tracking-leader of unknown control input and switching topologies. At present, the research on formation-containment tracking control for unmanned aerial vehicle swarm systems with a tracking-leader of unknown control input and switching topologies is still in its infancy, and there are few related research results[35].

Motivated by the above observations, this paper investigates the formation-containment tracking control for multi-UAV systems with switching topologies and unknown control inputs. Compared with the existing research results, the main contributions of this paper are threefold. First, the states of the formation-leaders are not only required to achieve the predefined time-varying formation but also need to track the state of the tracking-leader, and the followers need to converge to the convex hull spanned by the formation-leaders, which can control the macroscopic movement of the entire multi-UAV swarm system efficiently. Second, the interaction topology among the UAVs can be switched, which improves the practical application of multi-UAV swarm system. Third, a time-varying formation-containment tracking control protocol is proposed to compensate for the leader's unknown control input, and the feasible conditions given in this paper are more general.

The rest of this paper is organized as follows. Basic graph theory and problem description are given in Section 1. In Section 2, the main results are presented. In Section 3, the numerical simulation results are given. Conclusions are proposed in Section 4.

Notations: $\mathbf{R}^N$ stands for the N-dimension real column vector space and $\mathbf{R}^{N\times N}$ denotes the set of $N \times N$ dimensional real matrices. Let $\mathbf{1}_N$ be a column vector consisting of 1 with size N. $\boldsymbol{I}_N$ stands for an identity matrix with dimension N. $\otimes$ is the Kronecker product. Let $\mathrm{diag}(\cdot)$ represent a diagonal matrix and $\|\cdot\|$ stand for the 2-norm of a vector.

1 Preliminaries and Problem Description

1.1 Basic Graph Theory

Let $G = (v, e, \boldsymbol{w})$ be a directed graph with N nodes, where $v = \{v_1, v_2, \cdots, v_N\}$ represents the node set, the edge set is denoted by $e \subseteq \{(v_i, v_j) : v_i, v_j \in v(G); i \neq j\}$ and the weighted adjacency matrix is $\boldsymbol{w} = [w_{ij}] \in \mathbf{R}^{N\times N}$. For $\forall i, j \in \{1, 2, \cdots, N\}$, $w_{ij} > 0$ if and only if $(v_i, v_j) \in e$ and $w_{ij} = 0$ otherwise. The in-degree of node v_i is denoted by $\deg_{\rm in}(v_i) = \sum_{j=1}^{N} w_{ij}$. The degree matrix of G is represented by $\boldsymbol{D}(G) = \mathrm{diag}\{\deg_{\rm in}(v_1), \deg_{\rm in}(v_2), \cdots, \deg_{\rm in}(v_N)\}$. The Laplacian matrix is $\boldsymbol{L} = \boldsymbol{D} - \boldsymbol{w}$. And the neighbor set of vertex v_i is denoted by $N_i = \{v_j \in v : (v_i, v_j) \in e\}$. If a graph G has at least one root vertex and this vertex has a path with all other vertices, it is called a spanning tree.

Herein, the topologies among UAVs can be switched. All possible communication topologies of this system can be denoted by $\varGamma$, and the topological index set can be written as $\varDelta \subset \{1, 2, \cdots, N\}$. Let $\sigma(t) : [0, \infty) \to \varDelta$ be a switching signal and its value is the index of the topology at t. The graph and Laplacian matrix at t can be represented by $\bar{G}_{\sigma(t)}$ and $\boldsymbol{L}_{\sigma(t)}$. Let $N^i_{\sigma(t)}$ be the neighboring set of the UAV i at $\sigma(t)$. The interaction strength related to the edge from v_j to v_i is w_{ij}. And it is supposed that the admissible switching signal has a dwell time $T_{\rm d} > 0$.

Remark 1 Time-varying formation-containment tracking control problem for UAV swarm systems with switching interaction topologies is studied in this paper. These studies in Refs. [28-34] do not consider the switching topologies; however, in the actual flight process, the topology between UAVs is limited by the communication distance and the complex terrain environment, which may lead to the failure of communication links and the generation of new communication links, and then change the connectivity of the UAV swarm systems and the interaction relationship between the UAVs. In addition, the cooperative control problems for multi-agent systems with switching topologies are more complicated and challenging than the fixed cases[36]. Therefore, it is necessary to consider the condition of switching topologies in time-varying formation-containment tracking control.

1.2 Problem Description

Consider a UAV swarm system consisting of $N+M+1$ UAVs, where the tracking-leader is labeled by $i = 0$, the formation-leaders are denoted by $i = 1, 2, \cdots, N$, and the followers are represented by $i = N+1, N+2, \cdots, N+M$.

Remark 2 According to the collaborative task requirements, the UAVs are divided into tracking-leader, formation-leaders and followers. The formation-leaders are required to accomplish a predefined time-varying formation and track the desired trajectory of the tracking-leader, and the states of followers should converge to the convex hull spanned by those of the formation-leaders. Furthermore, the tracking-leader does not have a neighbor, and a formation-leader only has followers as its neighbors. The neighbor of followers only has formation-leaders or other followers.

Assumption 1 The directed graph $\bar{G}_{\sigma(t)}$ among the tracking-leader and formation-leaders has a spanning tree, and takes the tracking-leader as the root node.

Assumption 2 For each follower, there exists at least one formation-leader which has a directed path to it.

If Assumption 1 is satisfied, the Laplacian matrix $\boldsymbol{L}_{\sigma(t)} \in \mathbf{R}^{(N+M+1)\times(N+M+1)}$ has the following form:
$$\boldsymbol{L}_{\sigma(t)} = \begin{bmatrix} \mathbf{0} & \mathbf{0}_{1\times N} & \mathbf{0}_{1\times M} \\ \boldsymbol{L}_{12} & \boldsymbol{L}_{11} & \mathbf{0}_{N\times M} \\ \mathbf{0}_{M\times 1} & \boldsymbol{L}_2 & \boldsymbol{L}_3 \end{bmatrix},$$ where $\boldsymbol{L}_{12} \in \mathbf{R}^{N\times 1}$ denotes the Laplacian matrix among the formation-leaders and tracking-leader, $\boldsymbol{L}_{11} \in \mathbf{R}^{N\times N}$ represents the Laplacian matrix among formation-leaders and formation-leaders, $\boldsymbol{L}_2 \in \mathbf{R}^{M\times N}$ denotes the Laplacian matrix among the followers and formation-leaders, and $\boldsymbol{L}_3 \in \mathbf{R}^{M\times M}$ represents the Laplacian matrix among followers and followers.

Based on Assumptions 1 and 2, the following lemmas are given.

Lemma 1[32] Under Assumption 1, all eigenvalues of $\boldsymbol{L}_{11}$ have positive real parts.

Lemma 2[33] Under Assumption 2, all eigenvalues of $\boldsymbol{L}_3$ have positive real parts and each entry of $-\boldsymbol{L}_3^{-1}\boldsymbol{L}_2$ is nonnegative. Moreover, each row of $-\boldsymbol{L}_3^{-1}\boldsymbol{L}_2$ has a sum equal to one.

Lemma 3[34] Under Assumptions 1 and 2, there is a diagonal matrix $\boldsymbol{D}_{\rm L} = \mathrm{diag}(d_1, d_2, \cdots, d_N)$ with $d_i > 0\,(i = 1, 2, \cdots, N)$ such that $\boldsymbol{\varXi}_{\rm L} = \boldsymbol{D}_{\rm L}\boldsymbol{L}_{11} + \boldsymbol{L}_{11}^{\rm T}\boldsymbol{D}_{\rm L} > \mathbf{0}$, and there exists a diagonal matrix $\boldsymbol{G}_{\rm f} = \mathrm{diag}(g_1, g_2, \cdots, g_M)$ with $g_j > 0\,(j = 1, 2, \cdots, M)$ such that $\boldsymbol{\varPhi}_{\rm f} = \boldsymbol{G}_{\rm f}\boldsymbol{L}_3 + \boldsymbol{L}_3^{\rm T}\boldsymbol{G}_{\rm f} > \mathbf{0}$. Feasible matrices $\boldsymbol{D}_{\rm L}$ and $\boldsymbol{G}_{\rm f}$ can be calculated by $(d_1, d_2, \cdots, d_N)^{\rm T} = (\boldsymbol{L}_{11}^{\rm T})^{-1}\mathbf{1}_N$ and $(g_1, g_2, \cdots, g_M)^{\rm T} = (\boldsymbol{L}_3^{\rm T})^{-1}\mathbf{1}_M$.

The dynamics of the UAV swarm system can be decoupled into the position subsystem and the attitude subsystem, where the time constants for the position subsystem are much larger than the ones for the attitude subsystem. Therefore, the formation-containment tracking control for multi-UAV swarm systems can be classified into inner-loop control and outer-loop control, where the inner-loop controller is used to stabilize the attitude and the outer-loop controller is used to drive the UAV toward the desired position. This paper mainly considers the formation-containment tracking control for the outer-loop of UAV swarm system, and the position and velocity dynamics of the leaders and the followers in the outer loop can be approximately modelled, which will be given as follows.

The tracking-leader has a control input and the information of control input is unavailable to all the formation-leaders and followers. The dynamics of the tracking-leader can be written as

$$\left.\begin{aligned}\dot{\boldsymbol{x}}_0(t) &= \boldsymbol{v}_0(t)\\ \dot{\boldsymbol{v}}_0(t) &= \boldsymbol{u}_0(t)\end{aligned}\right\}, \tag{1}$$

where $\boldsymbol{x}_0(t) \in \mathbf{R}^n$ is the position vector, $\boldsymbol{v}_0(t) \in \mathbf{R}^n$ denotes the velocity vector, and $\boldsymbol{u}_0(t) \in \mathbf{R}^n$ represents the control input vector of the tracking-leader. The unknown control input $\boldsymbol{u}_0(t)$ satisfies the following bounded assumption.

Assumption 3 The unknown control input $\boldsymbol{u}_0(t)$ is bounded, and there exists an unknown positive constant μ such that $\|\boldsymbol{u}_0(t)\| \leqslant \mu$.

The dynamics of the formation-leaders and followers of $i\,(i = 1, 2, \cdots, N + M)$ can be represented by

$$\left.\begin{aligned}\dot{\boldsymbol{x}}_i(t) &= \boldsymbol{v}_i(t)\\ \dot{\boldsymbol{v}}_i(t) &= \boldsymbol{u}_i(t)\end{aligned}\right\}, \tag{2}$$

where $\boldsymbol{x}_i(t) \in \mathbf{R}^n$, $\boldsymbol{v}_i(t) \in \mathbf{R}^n$ and $\boldsymbol{u}_i(t) \in \mathbf{R}^n$ are the position, velocity and control input respectively. Based on the Kronecker product, the results can also be extended to the high-dimensional situations.

The desired time-varying formation of the formation-leaders can be denoted by $\boldsymbol{h}_{\mathrm{L}}(t) = (\boldsymbol{h}_1^{\mathrm{T}}(t), \boldsymbol{h}_2^{\mathrm{T}}(t), \cdots, \boldsymbol{h}_N^{\mathrm{T}}(t))^{\mathrm{T}}$, where $\boldsymbol{h}_i(t) = (\boldsymbol{h}_{ix}(t), \boldsymbol{h}_{iv}(t))^{\mathrm{T}}$, $i \in \{1, 2, \cdots, N\}$ are piecewise continuously differentiable vectors, and $\boldsymbol{h}_{ix}(t)$, $\boldsymbol{h}_{iv}(t)$ are the position and velocity components of $\boldsymbol{h}_i(t)$, respectively.

Remark 3 This paper considers the formation-containment tracking control problem when the formation-leaders have unknown control input. Compared with Ref. [28], the formation-leaders with unknown control input can complete the more complex task and cannot limit the type of reference signals generated by the tracking-leader, such as enclosing the target using a group of mobile robots in Ref. [37]. Furthermore, these works in Refs. [30-34] have introduced the formation-containment tracking control for general multi-agent systems with unknown control input, but the design of the formation-containment tracking feasible constraint is more complex. In this paper, based on the relative information of the neighboring UAVs and feasibility conditions, a distributed formation-containment tracking control protocol is designed, which can effectively make the design of the control protocol not rely on the boundary information of control input.

Let $\boldsymbol{\xi}_k(t) = (\boldsymbol{x}_k(t), \boldsymbol{v}_k(t))^{\mathrm{T}} (k = 0, 1, \cdots, N + M)$. Then the multi-UAV systems formed by Eqs. (1) and (2) can be written as

$$\left.\begin{aligned}\dot{\boldsymbol{\xi}}_0(t) &= \boldsymbol{A}\boldsymbol{\xi}_0(t) + \boldsymbol{B}\boldsymbol{u}_0(t)\\ \dot{\boldsymbol{\xi}}_i(t) &= \boldsymbol{A}\boldsymbol{\xi}_i(t) + \boldsymbol{B}\boldsymbol{u}_i(t)\end{aligned}\right\}, \tag{3}$$

where $\boldsymbol{A} = \begin{bmatrix}\mathbf{0}_{n\times n} & \boldsymbol{I}_{n\times n}\\ \mathbf{0}_{n\times n} & \mathbf{0}_{n\times n}\end{bmatrix}$ and $\boldsymbol{B} = \begin{bmatrix}\mathbf{0}_{n\times n}\\ \boldsymbol{I}_{n\times n}\end{bmatrix}$.

Definition 1 For any given initial states,

$$\lim_{t\to\infty} (\boldsymbol{\xi}_i(t) - \boldsymbol{h}_i(t) - \boldsymbol{\xi}_0(t)) = \mathbf{0}, \quad i = 1, 2, \cdots, N, \tag{4}$$

then the UAV swarm system (3) can achieve the time-varying formation tracking performance.

Definition 2 For the follower $c\,(c \in \{N + 1, N + 2, \cdots, N + M\})$ and any bounded initial states, there exists a nonnegative constant ι_0. If there exist nonnegative constants $a_{cj}\ (j = 1, 2, \cdots, N)$ satisfying $\sum\limits_{j=1}^{N} a_{cj} = 1$, such that

$$\lim_{t\to\infty} \left|\boldsymbol{\xi}_c(t) - \sum_{j=1}^{N} a_{cj}\boldsymbol{\xi}_j(t)\right| = \iota_0, \quad c = N + 1, N + 2, \cdots, N + M, \tag{5}$$

then the multi-UAV system is said to accomplish the containment.

Definition 3 For any bounded initial states, if (4) and (5) hold simultaneously for each formation-leader $i\,(i \in \{1, 2, \cdots, N\})$ and follower $c\,(c \in \{N + 1, N + 2, \cdots, N + M\})$, then the UAV swarm system is said to accomplish formation-containment tracking.

2 Main Results

In this section, the time-varying formation-containment tracking control protocol and the feasibility condition are proposed. And the proof will be given based on Lyapunov stability theory.

The local error of time-varying formation tracking for the formation-leader $i \in \{1, 2, \cdots, N\}$ can be written as

$$\boldsymbol{s}_i(t) = w_{i0}(\boldsymbol{\xi}_i(t) - \boldsymbol{h}_i(t) - \boldsymbol{\xi}_0(t)) + \sum_{j=1}^{N} w_{ij}((\boldsymbol{\xi}_i(t) - \boldsymbol{h}_i(t)) - (\boldsymbol{\xi}_j(t) - \boldsymbol{h}_j(t))). \tag{6}$$

The weight $w_{i0} > 0$ if the formation-leader i contains the tracking-leader, and $w_{i0} = 0$ otherwise. In addition, the containment local error for the follower $c\,(c \in \{N + 1, N + 2, \cdots, N + M\})$ can be written as

$$\boldsymbol{\varsigma}_i(t) = \sum_{j=1}^{N+M} w_{cj}(\boldsymbol{\xi}_c(t) - \boldsymbol{\xi}_j(t)), \tag{7}$$

where w_{i0} represents the information between the tracking-leader and the formation-leaders, w_{ij} represents the information between the formation-leaders and the formation-leaders, and w_{cj} represents the information between the followers and the formation-leaders and other followers.

According to the local error of time-varying formation tracking and the containment local error in (6) and (7), the time-varying formation-containment tracking control protocols can be given by

$$\begin{aligned} \boldsymbol{u}_i(t) = & -\eta g_i(\boldsymbol{s}_i(t)) - \|\dot{\boldsymbol{h}}_{iv}(t)\| g_i(\boldsymbol{s}_i(t)) - \\ & \alpha_1 \boldsymbol{B}^{\mathrm{T}} \boldsymbol{P} \boldsymbol{s}_i(t), \qquad (8) \\ & i \in \{1, 2, \cdots, N\}, \\ \boldsymbol{u}_i(t) = & -\alpha_2 \boldsymbol{B}^{\mathrm{T}} \boldsymbol{P} \boldsymbol{\varsigma}_i(t) - \omega g_i(\boldsymbol{\varsigma}_i(t)), \qquad (9) \\ & i \in \{N+1, N+2, \cdots, N+M\}, \end{aligned}$$

where η and ω are the positive constants, $g_i(\boldsymbol{s}_i(t))$ and $g_i(\boldsymbol{\varsigma}_i(t))$ denote the nonlinear functions, the positive constant $\alpha_1 \geqslant \dfrac{\lambda_{\max}(\boldsymbol{D}_{\mathrm{L}})}{\lambda_{\min}(\boldsymbol{\varXi}_{\mathrm{L}})}$, and $\alpha_2 \geqslant \dfrac{\lambda_{\max}(\boldsymbol{G}_{\mathrm{f}})}{\lambda_{\min}(\boldsymbol{\varPhi}_{\mathrm{f}})}$. In addition, positive definite matrix $\boldsymbol{P}$ satisfies the following algebraic Riccati equation:

$$\boldsymbol{A}^{\mathrm{T}} \boldsymbol{P} + \boldsymbol{P} \boldsymbol{A} - \boldsymbol{P} \boldsymbol{B} \boldsymbol{B}^{\mathrm{T}} \boldsymbol{P} + \boldsymbol{I} \leqslant \boldsymbol{0}. \qquad (10)$$

The non-linear functions $g_i(\boldsymbol{s}_i(t))$ and $g_i(\boldsymbol{\varsigma}_i(t))$ are written as

$$g_i(\boldsymbol{s}_i(t)) = \begin{cases} \dfrac{\boldsymbol{B}^{\mathrm{T}} \boldsymbol{P} \boldsymbol{s}_i(t)}{\|\boldsymbol{B}^{\mathrm{T}} \boldsymbol{P} \boldsymbol{s}_i(t)\|}, & \|\boldsymbol{B}^{\mathrm{T}} \boldsymbol{P} \boldsymbol{s}_i(t)\| \neq 0 \\ 0, & \|\boldsymbol{B}^{\mathrm{T}} \boldsymbol{P} \boldsymbol{s}_i(t)\| = 0 \end{cases}, \qquad (11)$$

$$g_i(\boldsymbol{\varsigma}_i(t)) = \begin{cases} \dfrac{\boldsymbol{B}^{\mathrm{T}} \boldsymbol{P} \boldsymbol{\varsigma}_i(t)}{\|\boldsymbol{B}^{\mathrm{T}} \boldsymbol{P} \boldsymbol{\varsigma}_i(t)\|}, & \|\boldsymbol{B}^{\mathrm{T}} \boldsymbol{P} \boldsymbol{\varsigma}_i(t)\| \neq 0 \\ 0, & \|\boldsymbol{B}^{\mathrm{T}} \boldsymbol{P} \boldsymbol{\varsigma}_i(t)\| = 0 \end{cases}. \qquad (12)$$

Theorem 1 For the UAV swarm system (3), if Assumptions 1—3 hold and the time-varying formation $\boldsymbol{h}_{\mathrm{L}}(t)$ meets the feasibility condition $\dot{\boldsymbol{h}}_{ix}(t) - \boldsymbol{h}_{iv}(t) = \boldsymbol{0}$, $i \in \{1, 2, \cdots, N\}$, and the positive definite matrix $\boldsymbol{P}$ satisfies Inequality (10), the time-varying formation-containment tracking performance defined by (4) and (5) for the multi-UAV system (3) with the tracking-leader's unknown control input can be achieved by using the control protocols (8) and (9).

Proof By substituting the control protocols (8) and (9) into the multi-UAV systems (3), then one can get the following compact forms:

$$\begin{aligned} \dot{\boldsymbol{\xi}}_{\mathrm{L}}(t) = & (\boldsymbol{I}_N \otimes \boldsymbol{A}) \boldsymbol{\xi}_{\mathrm{L}}(t) - \eta (\boldsymbol{I}_N \otimes \boldsymbol{B}) G(\boldsymbol{s}(t)) - \\ & (\boldsymbol{\varPi} \otimes \boldsymbol{B}) G(\boldsymbol{s}(t)) - \alpha_1 (\boldsymbol{I}_N \otimes \boldsymbol{B} \boldsymbol{B}^{\mathrm{T}} \boldsymbol{P}) \boldsymbol{s}(t), \qquad (13) \\ \dot{\boldsymbol{\xi}}_{\mathrm{F}}(t) = & (\boldsymbol{I}_M \otimes \boldsymbol{A}) \boldsymbol{\xi}_{\mathrm{F}}(t) - \alpha_2 (\boldsymbol{I}_M \otimes \boldsymbol{B} \boldsymbol{B}^{\mathrm{T}} \boldsymbol{P}) \boldsymbol{\varsigma}(t) - \\ & \omega (\boldsymbol{I}_M \otimes \boldsymbol{B}) G(\boldsymbol{\varsigma}(t)), \qquad (14) \end{aligned}$$

where $\boldsymbol{\xi}_{\mathrm{L}}(t) = (\boldsymbol{\xi}_1^{\mathrm{T}}(t), \boldsymbol{\xi}_2^{\mathrm{T}}(t), \cdots, \boldsymbol{\xi}_N^{\mathrm{T}}(t))^{\mathrm{T}}$, $\boldsymbol{\xi}_{\mathrm{F}}(t) = (\boldsymbol{\xi}_{N+1}^{\mathrm{T}}(t), \boldsymbol{\xi}_{N+2}^{\mathrm{T}}(t), \cdots, \boldsymbol{\xi}_{N+M}^{\mathrm{T}}(t))^{\mathrm{T}}$, $\boldsymbol{s}(t) = (\boldsymbol{s}_1^{\mathrm{T}}(t), \boldsymbol{s}_2^{\mathrm{T}}(t), \cdots, \boldsymbol{s}_N^{\mathrm{T}}(t))^{\mathrm{T}}$ and $\boldsymbol{\varsigma}(t) = (\boldsymbol{\varsigma}_{N+1}^{\mathrm{T}}(t), \boldsymbol{\varsigma}_{N+2}^{\mathrm{T}}(t), \cdots, \boldsymbol{\varsigma}_{N+M}^{\mathrm{T}}(t))^{\mathrm{T}}$, $\boldsymbol{\varPi}(t) = \mathrm{diag}(\|\dot{\boldsymbol{h}}_{1v}(t)\|, \|\dot{\boldsymbol{h}}_{2v}(t)\|, \cdots, \|\dot{\boldsymbol{h}}_{Nv}(t)\|)^{\mathrm{T}}$, $G(\boldsymbol{s}(t)) = (g_1^{\mathrm{T}}(\boldsymbol{s}_1(t)), g_2^{\mathrm{T}}(\boldsymbol{s}_2(t)), \cdots, g_N^{\mathrm{T}}(\boldsymbol{s}_N(t)))^{\mathrm{T}}$, $G(\boldsymbol{\varsigma}(t)) = (g_{N+1}^{\mathrm{T}}(\boldsymbol{\varsigma}_{N+1}(t)), g_{N+2}^{\mathrm{T}}(\boldsymbol{\varsigma}_{N+2}(t)), \cdots, g_{N+M}^{\mathrm{T}}(\boldsymbol{\varsigma}_{N+M}(t)))^{\mathrm{T}}$.

The time-varying formation tracking error of the formation-leader i ($i = 1, 2, \cdots, N$) can be expressed by $\boldsymbol{\psi}_i(t) = \boldsymbol{\xi}_i(t) - \boldsymbol{h}_i(t) - \boldsymbol{\xi}_0(t)$. By taking the derivative of $\boldsymbol{\psi}_i(t)$ along the trajectory of system (3) and considering the control protocol (8),

$$\begin{aligned} \dot{\boldsymbol{\psi}}_i(t) = & \dot{\boldsymbol{\xi}}_i(t) - \dot{\boldsymbol{h}}_i(t) - \dot{\boldsymbol{\xi}}_0(t) = \\ & \boldsymbol{A} \boldsymbol{\xi}_i(t) + \boldsymbol{B} \boldsymbol{u}_i(t) - \dot{\boldsymbol{h}}_i(t) - \boldsymbol{A} \boldsymbol{\xi}_0(t) - \boldsymbol{B} \boldsymbol{u}_0(t) = \\ & \boldsymbol{A} \boldsymbol{\xi}_i(t) + \boldsymbol{B}(-\eta g_i(\boldsymbol{s}_i(t)) - \\ & \|\dot{\boldsymbol{h}}_{iv}(t)\| g_i(\boldsymbol{s}_i(t)) - \alpha_1 \boldsymbol{B}^{\mathrm{T}} \boldsymbol{P} \boldsymbol{s}_i(t)) - \\ & \dot{\boldsymbol{h}}_i(t) - \boldsymbol{A} \boldsymbol{\xi}_0(t) - \boldsymbol{B} \boldsymbol{u}_0(t) - \boldsymbol{A} \boldsymbol{h}_i(t) + \boldsymbol{A} \boldsymbol{h}_i(t) = \\ & \boldsymbol{A} \boldsymbol{\psi}_i(t) - \boldsymbol{B} \eta g_i(\boldsymbol{s}_i(t)) - \boldsymbol{B} \|\dot{\boldsymbol{h}}_{iv}(t)\| g_i(\boldsymbol{s}_i(t)) - \\ & \alpha_1 \boldsymbol{B} \boldsymbol{B}^{\mathrm{T}} \boldsymbol{P} \boldsymbol{s}_i(t) - \dot{\boldsymbol{h}}_i(t) + \boldsymbol{A} \boldsymbol{h}_i(t). \qquad (15) \end{aligned}$$

According to the fact that the given time-varying formation meets the feasibility condition: $\dot{\boldsymbol{h}}_{ix}(t) - \boldsymbol{h}_{iv}(t) = \boldsymbol{0}$, let $\boldsymbol{\psi}(t) = (\boldsymbol{\psi}_1^{\mathrm{T}}(t), \boldsymbol{\psi}_2^{\mathrm{T}}(t), \cdots, \boldsymbol{\psi}_N^{\mathrm{T}}(t))^{\mathrm{T}}$, $\boldsymbol{h}_v(t) = (\boldsymbol{h}_{1v}(t), \boldsymbol{h}_{2v}(t), \cdots, \boldsymbol{h}_{Nv}(t))^{\mathrm{T}}$, $\boldsymbol{\varPi}(t) = \mathrm{diag}(\|\dot{\boldsymbol{h}}_{1v}(t)\|, \|\dot{\boldsymbol{h}}_{2v}(t)\|, \cdots, \|\dot{\boldsymbol{h}}_{Nv}(t)\|)^{\mathrm{T}}$. Then the UAV swarm system can be written by

$$\begin{aligned} \dot{\boldsymbol{\psi}}(t) = & (\boldsymbol{I}_N \otimes \boldsymbol{A}) \boldsymbol{\psi}(t) - (\boldsymbol{I}_N \otimes \boldsymbol{B}) \dot{\boldsymbol{h}}_v(t) - \\ & \eta (\boldsymbol{I}_N \otimes \boldsymbol{B}) G(\boldsymbol{s}(t)) - (\boldsymbol{\varPi} \otimes \boldsymbol{B}) G(\boldsymbol{s}(t)) - \\ & \alpha_1 (\boldsymbol{I}_N \otimes \boldsymbol{B} \boldsymbol{B}^{\mathrm{T}} \boldsymbol{P}) \boldsymbol{s}(t) - (\boldsymbol{I}_N \otimes \boldsymbol{B}) \boldsymbol{u}_0(t). \qquad (16) \end{aligned}$$

The neighbor errors $\boldsymbol{s}(t)$ and $\boldsymbol{\varsigma}(t)$ can described by $\boldsymbol{s}(t) = (\boldsymbol{L}_{11} \otimes \boldsymbol{I}_2) \boldsymbol{\psi}(t)$ and $\boldsymbol{\varsigma}(t) = (\boldsymbol{L}_3 \otimes \boldsymbol{I}_n)(\boldsymbol{\xi}_{\mathrm{F}}(t) - (-\boldsymbol{L}_3^{-1} \boldsymbol{L}_2 \otimes \boldsymbol{I}_n) \boldsymbol{\xi}_{\mathrm{L}}(t))$. Then one gets the following compact form:

$$\begin{aligned} \dot{\boldsymbol{s}}(t) = & (\boldsymbol{I}_N \otimes \boldsymbol{A}) \boldsymbol{s}(t) - (\boldsymbol{L}_{11} \otimes \boldsymbol{B}) \dot{\boldsymbol{h}}_{\boldsymbol{v}}(t) - \\ & \eta (\boldsymbol{L}_{11} \otimes \boldsymbol{B}) G(\boldsymbol{s}(t)) - (\boldsymbol{L}_{11} \boldsymbol{\varPi} \otimes \boldsymbol{B}) G(\boldsymbol{s}(t)) - \\ & \alpha_1 (\boldsymbol{L}_{11} \otimes \boldsymbol{B} \boldsymbol{B}^{\mathrm{T}} \boldsymbol{P}) \boldsymbol{s}(t) - (\boldsymbol{L}_{11} \otimes \boldsymbol{B}) \boldsymbol{u}_0(t). \qquad (17) \end{aligned}$$

Considering the following Lyapunov function:

$$\boldsymbol{V}_1(t) = \boldsymbol{s}^{\mathrm{T}}(t)(\boldsymbol{D}_{\mathrm{L}} \otimes \boldsymbol{P}) \boldsymbol{s}(t), \qquad (18)$$

where $\boldsymbol{D}_{\mathrm{L}}$ is a positive diagonal matrix defined in Lemma 3, then the derivative of $\boldsymbol{V}_1(t)$ yields

$$\begin{aligned} \dot{\boldsymbol{V}}_1(t) = & \boldsymbol{s}^{\mathrm{T}}(t)(\boldsymbol{D}_{\mathrm{L}} \otimes (\boldsymbol{P} \boldsymbol{A} + \boldsymbol{A}^{\mathrm{T}} \boldsymbol{P})) \boldsymbol{s}(t) - \\ & 2 \boldsymbol{s}^{\mathrm{T}}(t)(\boldsymbol{D}_{\mathrm{L}} \boldsymbol{L}_{11} \otimes \boldsymbol{P} \boldsymbol{B}) \dot{\boldsymbol{h}}_v(t) - \\ & 2 \eta \boldsymbol{s}^{\mathrm{T}}(t)(\boldsymbol{D}_{\mathrm{L}} \boldsymbol{L}_{11} \otimes \boldsymbol{P} \boldsymbol{B}) G(\boldsymbol{s}(t)) - \\ & 2 \boldsymbol{s}^{\mathrm{T}}(t)(\boldsymbol{D}_{\mathrm{L}} \boldsymbol{L}_{11} \boldsymbol{\varPi} \otimes \boldsymbol{P} \boldsymbol{B}) G(\boldsymbol{s}(t)) - \\ & \alpha_1 \boldsymbol{s}^{\mathrm{T}}(t)(\boldsymbol{\varXi}_{\mathrm{L}} \otimes \boldsymbol{P} \boldsymbol{B} \boldsymbol{B}^{\mathrm{T}} \boldsymbol{P}) \boldsymbol{s}(t) - \\ & 2 \boldsymbol{s}^{\mathrm{T}}(t)(\boldsymbol{D}_{\mathrm{L}} \boldsymbol{L}_{11} \otimes \boldsymbol{P} \boldsymbol{B}) \boldsymbol{u}_0(t), \qquad (19) \end{aligned}$$

where $\boldsymbol{\Xi}_\mathrm{L} = \boldsymbol{D}_\mathrm{L}\boldsymbol{L}_{11} + \boldsymbol{L}_{11}^\mathrm{T}\boldsymbol{D}_\mathrm{L} > \boldsymbol{0}$.

$$\begin{aligned}&-2\boldsymbol{s}^\mathrm{T}(t)(\boldsymbol{D}_\mathrm{L}\boldsymbol{L}_{11}\otimes\boldsymbol{PB})\dot{\boldsymbol{h}}_v(t) = \\ &\quad -2\sum_{i=1}^N d_i w_{i0}\boldsymbol{s}_i^\mathrm{T}\boldsymbol{PB}\dot{\boldsymbol{h}}_{iv} \leqslant \\ &\quad 2\sum_{i=1}^N d_i w_{i0}\|\boldsymbol{B}^\mathrm{T}\boldsymbol{P}\boldsymbol{s}_i\|\|\dot{\boldsymbol{h}}_{iv}\|,\end{aligned} \tag{20}$$

$$\begin{aligned}&-2\eta\boldsymbol{s}^\mathrm{T}(t)(\boldsymbol{D}_\mathrm{L}\boldsymbol{L}_{11}\otimes\boldsymbol{PB})G(\boldsymbol{s}(t)) = \\ &\quad -2\eta\sum_{i=1}^N d_i\boldsymbol{s}_i^\mathrm{T}\boldsymbol{PB}\Big(\sum_{j=1}^N w_{ij}(g(\boldsymbol{s}_i)-g(\boldsymbol{s}_j))+ \\ &\quad w_{i0}g(\boldsymbol{s}_i)\Big) \leqslant -2\eta\sum_{i=1}^N d_i w_{i0}\|\boldsymbol{B}^\mathrm{T}\boldsymbol{P}\boldsymbol{s}_i\|,\end{aligned} \tag{21}$$

$$\begin{aligned}&-2\boldsymbol{s}^\mathrm{T}(t)(\boldsymbol{D}_\mathrm{L}\boldsymbol{L}_{11}\boldsymbol{\Pi}\otimes\boldsymbol{PB})G(\boldsymbol{s}(t)) = \\ &\quad -2\sum_{i=1}^N d_i\boldsymbol{s}_i^\mathrm{T}\boldsymbol{PB}\|\dot{\boldsymbol{h}}_{iv}\|\Big(\sum_{j=1}^N w_{ij}(g(\boldsymbol{s}_i)- \\ &\quad g(\boldsymbol{s}_j))+w_{i0}g(\boldsymbol{s}_i)\Big) \leqslant \\ &\quad -2\sum_{i=1}^N d_i w_{i0}\|\dot{\boldsymbol{h}}_{iv}\|\|\boldsymbol{B}^\mathrm{T}\boldsymbol{P}\boldsymbol{s}_i\|,\end{aligned} \tag{22}$$

$$\begin{aligned}&-2\boldsymbol{s}^\mathrm{T}(t)(\boldsymbol{D}_\mathrm{L}\boldsymbol{L}_{11}\otimes\boldsymbol{PB})\boldsymbol{u}_0(t) = \\ &\quad -2\sum_{i=1}^N d_i w_{i0}\boldsymbol{s}_i^\mathrm{T}\boldsymbol{PB}\boldsymbol{u}_0 \leqslant \\ &\quad 2\sum_{i=1}^N d_i w_{i0}\|\boldsymbol{B}^\mathrm{T}\boldsymbol{P}\boldsymbol{s}_i\|\|\boldsymbol{u}_0\| \leqslant \\ &\quad 2\mu\sum_{i=1}^N d_i w_{i0}\|\boldsymbol{B}^\mathrm{T}\boldsymbol{P}\boldsymbol{s}_i\|.\end{aligned} \tag{23}$$

Substituting (20)—(23) into (19) yields

$$\begin{aligned}\dot{\boldsymbol{V}}_1(t) \leqslant{}& \boldsymbol{s}^\mathrm{T}(t)(\boldsymbol{D}_\mathrm{L}\otimes(\boldsymbol{PA}+\boldsymbol{A}^\mathrm{T}\boldsymbol{P}))\boldsymbol{s}(t)- \\ & \alpha_1\boldsymbol{s}^\mathrm{T}(t)(\boldsymbol{\Xi}_\mathrm{L}\otimes\boldsymbol{PBB}^\mathrm{T}\boldsymbol{P})\boldsymbol{s}(t)+ \\ & 2\sum_{i=1}^N d_i w_{i0}\|\boldsymbol{B}^\mathrm{T}\boldsymbol{P}\boldsymbol{s}_i\|\|\dot{\boldsymbol{h}}_{iv}\|- \\ & 2\eta\sum_{i=1}^N d_i w_{i0}\|\boldsymbol{B}^\mathrm{T}\boldsymbol{P}\boldsymbol{s}_i\|- \\ & 2\sum_{i=1}^N d_i w_{i0}\|\dot{\boldsymbol{h}}_{iv}\|\|\boldsymbol{B}^\mathrm{T}\boldsymbol{P}\boldsymbol{s}_i\|+ \\ & 2\mu\sum_{i=1}^N d_i w_{i0}\|\boldsymbol{B}^\mathrm{T}\boldsymbol{P}\boldsymbol{s}_i\| \leqslant \\ & \boldsymbol{s}^\mathrm{T}(t)(\boldsymbol{D}_\mathrm{L}\otimes(\boldsymbol{PA}+\boldsymbol{A}^\mathrm{T}\boldsymbol{P}))\boldsymbol{s}(t)- \\ & \alpha_1\boldsymbol{s}^\mathrm{T}(t)(\boldsymbol{\Xi}_\mathrm{L}\otimes\boldsymbol{PBB}^\mathrm{T}\boldsymbol{P})\boldsymbol{s}(t)- \\ & 2(\eta-\mu)\sum_{i=1}^N d_i w_{i0}\|\boldsymbol{B}^\mathrm{T}\boldsymbol{P}\boldsymbol{s}_i\|.\end{aligned} \tag{24}$$

Choose $\alpha_1 \geqslant \dfrac{\lambda_{\max}(\boldsymbol{D}_\mathrm{L})}{\lambda_{\min}(\boldsymbol{\Xi}_\mathrm{L})}$ and $\eta \geqslant \mu$. Then it holds from (24) that

$$\begin{aligned}\dot{\boldsymbol{V}}_1(t) \leqslant{}& \boldsymbol{s}^\mathrm{T}(t)(\boldsymbol{D}_\mathrm{L}\otimes \\ & (\boldsymbol{PA}+\boldsymbol{A}^\mathrm{T}\boldsymbol{P}-\boldsymbol{PBB}^\mathrm{T}\boldsymbol{P}))\boldsymbol{s}(t).\end{aligned} \tag{25}$$

If inequality $\boldsymbol{PA}+\boldsymbol{A}^\mathrm{T}\boldsymbol{P}-\boldsymbol{PBB}^\mathrm{T}\boldsymbol{P}+\boldsymbol{I}\leqslant\boldsymbol{0}$ holds, then it can be verified that

$$\dot{\boldsymbol{V}}_1 \leqslant -\sum_{i=1}^N d_i\boldsymbol{s}_i^\mathrm{T}(t)\boldsymbol{s}_i(t) \leqslant \boldsymbol{0}. \tag{26}$$

Therefore, the Lyapunov function $\boldsymbol{V}_1(t)$ is asymptotically stable according to LaSalle's invariance principle. It can be obtained that $\lim\limits_{t\to\infty}\boldsymbol{s}_i(t)=\boldsymbol{0}$, because of $\boldsymbol{s}(t) = (\boldsymbol{L}_{11}\otimes\boldsymbol{I}_2)\boldsymbol{\psi}(t)$, then one gets $\lim\limits_{t\to\infty}\boldsymbol{\psi}_i(t)=\boldsymbol{0}$. Based on above analyses, the UAV swarm system (3) can achieve the desired time-varying formation tracking under the control protocol (8) based on Definition 1.

According to the neighbor error $\boldsymbol{\varsigma}(t) = (\boldsymbol{L}_3\otimes\boldsymbol{I}_n)(\boldsymbol{\xi}_\mathrm{F}(t)-(-\boldsymbol{L}_3^{-1}\boldsymbol{L}_2\otimes\boldsymbol{I}_n)\boldsymbol{\xi}_\mathrm{L}(t))$, one can obtain

$$\begin{aligned}\dot{\boldsymbol{\varsigma}}(t) ={}& (\boldsymbol{L}_3\otimes\boldsymbol{I}_n)(\dot{\boldsymbol{\xi}}_\mathrm{F}(t)-(-\boldsymbol{L}_3^{-1}\boldsymbol{L}_2\otimes\boldsymbol{I}_n)\dot{\boldsymbol{\xi}}_\mathrm{L}(t)) = \\ & (\boldsymbol{L}_3\otimes\boldsymbol{I}_n)[(\boldsymbol{I}_M\otimes\boldsymbol{A})\boldsymbol{\xi}_\mathrm{F}(t)-\alpha_2(\boldsymbol{I}_M\otimes \\ & \boldsymbol{BB}^\mathrm{T}\boldsymbol{P})\boldsymbol{\varsigma}(t)-\omega(\boldsymbol{I}_M\otimes\boldsymbol{B})G(\boldsymbol{\varsigma}(t))]+(\boldsymbol{L}_2\otimes\boldsymbol{I}_n) \\ & [(\boldsymbol{I}_N\otimes\boldsymbol{A})\boldsymbol{\xi}_L(t)-\eta(\boldsymbol{I}_N\otimes\boldsymbol{B})G(\boldsymbol{s}(t))- \\ & (\boldsymbol{I}_N\boldsymbol{\Pi}\otimes\boldsymbol{B})G(\boldsymbol{s}(t))-\alpha_1(\boldsymbol{I}_N\otimes\boldsymbol{BB}^\mathrm{T}\boldsymbol{P})\boldsymbol{s}(t)] = \\ & (\boldsymbol{I}_M\otimes\boldsymbol{A})\boldsymbol{\varsigma}(t)-\alpha_2(\boldsymbol{L}_3\otimes\boldsymbol{BB}^\mathrm{T}\boldsymbol{P})\boldsymbol{\varsigma}(t)- \\ & \omega(\boldsymbol{L}_3\otimes\boldsymbol{B})G(\boldsymbol{\varsigma}(t))-\eta(\boldsymbol{L}_2\otimes\boldsymbol{B})G(\boldsymbol{s}(t))- \\ & (\boldsymbol{L}_2\boldsymbol{\Pi}\otimes\boldsymbol{B})G(\boldsymbol{s}(t))-\alpha_1(\boldsymbol{L}_2\otimes\boldsymbol{BB}^\mathrm{T}\boldsymbol{P})\boldsymbol{s}(t).\end{aligned} \tag{27}$$

Herein, the following Lyapunov function candidate is considered:

$$\boldsymbol{V}_2(t) = \boldsymbol{\varsigma}^\mathrm{T}(t)(\boldsymbol{G}_\mathrm{f}\otimes\boldsymbol{P})\boldsymbol{\varsigma}(t). \tag{28}$$

Then the time derivative of $\boldsymbol{V}_2(t)$ is described by

$$\begin{aligned}\dot{\boldsymbol{V}}_2(t) ={}& \boldsymbol{\varsigma}^\mathrm{T}(t)(\boldsymbol{G}_\mathrm{f}\otimes(\boldsymbol{PA}+\boldsymbol{A}^\mathrm{T}\boldsymbol{P}))\boldsymbol{\varsigma}(t)- \\ & \alpha_2\boldsymbol{\varsigma}^\mathrm{T}(t)(\boldsymbol{\Phi}_\mathrm{f}\otimes\boldsymbol{PBB}^\mathrm{T}\boldsymbol{P})\boldsymbol{\varsigma}(t)- \\ & 2\omega\boldsymbol{\varsigma}^\mathrm{T}(t)(\boldsymbol{G}_\mathrm{f}\boldsymbol{L}_3\otimes\boldsymbol{PB})G(\boldsymbol{\varsigma}(t))- \\ & 2\eta\boldsymbol{\varsigma}^\mathrm{T}(t)(\boldsymbol{G}_\mathrm{f}\boldsymbol{L}_2\otimes\boldsymbol{PB})G(\boldsymbol{s}(t))- \\ & 2\boldsymbol{\varsigma}^\mathrm{T}(t)(\boldsymbol{G}_\mathrm{f}\boldsymbol{L}_2\boldsymbol{\Pi}\otimes\boldsymbol{PB})G(\boldsymbol{s}(t))- \\ & 2\alpha_1\boldsymbol{\varsigma}^\mathrm{T}(t)(\boldsymbol{G}_\mathrm{f}\boldsymbol{L}_2\otimes\boldsymbol{PBB}^\mathrm{T}\boldsymbol{P})\boldsymbol{s}(t),\end{aligned} \tag{29}$$

where $\boldsymbol{\Phi}_{\mathrm{f}} = \boldsymbol{G}_{\mathrm{f}}\boldsymbol{L}_3 + \boldsymbol{L}_3^{\mathrm{T}}\boldsymbol{G}_{\mathrm{f}} > \mathbf{0}$.

$$\begin{aligned}&-2\omega\boldsymbol{\varsigma}^{\mathrm{T}}(t)(\boldsymbol{G}_{\mathrm{f}}\boldsymbol{L}_3\otimes\boldsymbol{PB})G(\boldsymbol{\varsigma}(t)) = \\ &\quad -2\omega\sum_{i=N+1}^{N+M} g_i\boldsymbol{\varsigma}_i^{\mathrm{T}}\boldsymbol{PB}\Big(\sum_{j=N+1}^{N+M} w_{ij}(g(\boldsymbol{\varsigma}_i)- \\ &\quad g(\boldsymbol{\varsigma}_j)) + \sum_{k=1}^{N} w_{ik}g(\boldsymbol{\varsigma}_i)\Big) \leqslant \\ &\quad -2\omega\sum_{i=N+1}^{N+M} g_i\|\boldsymbol{B}^{\mathrm{T}}\boldsymbol{P}\boldsymbol{\varsigma}_i\|\sum_{k=1}^{N} w_{ik}.\end{aligned}\tag{30}$$

Let $\boldsymbol{E}(t) = (\boldsymbol{E}_1^{\mathrm{T}}(t), \boldsymbol{E}_2^{\mathrm{T}}(t), \cdots, \boldsymbol{E}_N^{\mathrm{T}}(t))^{\mathrm{T}}$ and $\boldsymbol{E}_i(t) = \eta G(\boldsymbol{s}_i(t)) + \|\dot{\boldsymbol{h}}_{iv}(t)\|G(\boldsymbol{s}_\iota(t))$ $(i \in 1, 2, \cdots, N)$. As $\boldsymbol{h}_i(t)$ and $\dot{\boldsymbol{h}}_i(t)$ are bounded, one can obtain that there are positive constants ε_i such that $\|\dot{\boldsymbol{h}}_{iv}(t)\| \leqslant \varepsilon_i$ $(i = 1, 2, \cdots, N)$. And given $\|G(\boldsymbol{s}_i(t))\| \leqslant 1$, it leads to $\|\boldsymbol{E}_i(t)\| \leqslant \varepsilon_i + \eta$. Then one gets

$$\begin{aligned}&-2\eta\boldsymbol{\varsigma}^{\mathrm{T}}(t)(\boldsymbol{G}_{\mathrm{f}}\boldsymbol{L}_2\otimes\boldsymbol{PB})G(\boldsymbol{s}(t))- \\ &\quad 2\boldsymbol{\varsigma}^{\mathrm{T}}(t)(\boldsymbol{G}_{\mathrm{f}}\boldsymbol{L}_2\boldsymbol{\Pi}\otimes\boldsymbol{PB})G(\boldsymbol{s}(t)) = \\ &\quad -2\boldsymbol{\varsigma}^{\mathrm{T}}(t)(\boldsymbol{G}_{\mathrm{f}}\boldsymbol{L}_2\otimes\boldsymbol{PB})(\eta G(\boldsymbol{s}(t))+ \\ &\quad \|\dot{\boldsymbol{h}}_v(t)\|G(\boldsymbol{s}(t))) = \\ &\quad 2\sum_{i=N+1}^{N+M} g_i\boldsymbol{\varsigma}_i^{\mathrm{T}}\boldsymbol{PB}\sum_{k=1}^{N} w_{ik}\boldsymbol{E}_k(t) \leqslant \\ &\quad 2\sum_{i=N+1}^{N+M} g_i\|\boldsymbol{B}^{\mathrm{T}}\boldsymbol{P}\boldsymbol{\varsigma}_i\|\sum_{k=1}^{N} w_{ik}\|\boldsymbol{E}_k(t)\| \leqslant \\ &\quad 2\gamma\sum_{i=N+1}^{N+M} g_i\|\boldsymbol{B}^{\mathrm{T}}\boldsymbol{P}\boldsymbol{\varsigma}_i\|\sum_{k=1}^{N} w_{ik},\end{aligned}\tag{31}$$

where $\gamma = \max\{\varepsilon_1, \varepsilon_2, \cdots, \varepsilon_N\} + \eta$.

Substituting (30) and (31) into (29) leads to

$$\begin{aligned}\dot{\boldsymbol{V}}_2(t) = &\,\boldsymbol{\varsigma}^{\mathrm{T}}(t)(\boldsymbol{G}_{\mathrm{f}}\otimes(\boldsymbol{PA}+\boldsymbol{A}^{\mathrm{T}}\boldsymbol{P}))\boldsymbol{\varsigma}(t)- \\ &\alpha_2\boldsymbol{\varsigma}^{\mathrm{T}}(t)(\boldsymbol{\Phi}_{\mathrm{f}}\otimes\boldsymbol{PBB}^{\mathrm{T}}\boldsymbol{P})\boldsymbol{\varsigma}(t)- \\ &2\omega\sum_{i=N+1}^{N+M} g_i\|\boldsymbol{B}^{\mathrm{T}}\boldsymbol{P}\boldsymbol{\varsigma}_i\|\sum_{k=1}^{N} w_{ik}+ \\ &2\gamma\sum_{i=N+1}^{N+M} g_i\|\boldsymbol{B}^{\mathrm{T}}\boldsymbol{P}\boldsymbol{\varsigma}_i\|\sum_{k=1}^{N} w_{ik}- \\ &2\alpha_1\boldsymbol{\varsigma}^{\mathrm{T}}(t)(\boldsymbol{G}_{\mathrm{f}}\boldsymbol{L}_2\otimes\boldsymbol{PBB}^{\mathrm{T}}\boldsymbol{P})\boldsymbol{s}(t) = \\ &\boldsymbol{\varsigma}^{\mathrm{T}}(t)(\boldsymbol{G}_{\mathrm{f}}\otimes(\boldsymbol{PA}+\boldsymbol{A}^{\mathrm{T}}\boldsymbol{P}))\boldsymbol{\varsigma}(t)- \\ &\alpha_2\boldsymbol{\varsigma}^{\mathrm{T}}(t)(\boldsymbol{\Phi}_{\mathrm{f}}\otimes\boldsymbol{PBB}^{\mathrm{T}}\boldsymbol{P})\boldsymbol{\varsigma}(t)- \\ &2(\omega-\gamma)\sum_{i=N+1}^{N+M} g_i\|\boldsymbol{B}^{\mathrm{T}}\boldsymbol{P}\boldsymbol{\varsigma}_i\|\sum_{k=1}^{N} w_{ik}- \\ &2\alpha_1\boldsymbol{\varsigma}^{\mathrm{T}}(t)(\boldsymbol{G}_{\mathrm{f}}\boldsymbol{L}_2\otimes\boldsymbol{PBB}^{\mathrm{T}}\boldsymbol{P})\boldsymbol{s}(t).\end{aligned}\tag{32}$$

Let $\alpha_2 \geqslant \dfrac{\lambda_{\max}(\boldsymbol{G}_{\mathrm{f}})}{\lambda_{\min}(\boldsymbol{\Phi}_{\mathrm{f}})}$ and $\omega \geqslant \gamma$. Then it can follow from (32) that

$$\begin{aligned}\dot{\boldsymbol{V}}_2(t) \leqslant &\,\boldsymbol{\varsigma}^{\mathrm{T}}(t)(\boldsymbol{G}_{\mathrm{f}}\otimes(\boldsymbol{PA}+\boldsymbol{A}^{\mathrm{T}}\boldsymbol{P}-\boldsymbol{PBB}^{\mathrm{T}}\boldsymbol{P}))\boldsymbol{\varsigma}(t)- \\ &2\alpha_1\boldsymbol{\varsigma}^{\mathrm{T}}(t)(\boldsymbol{G}_{\mathrm{f}}\boldsymbol{L}_2\otimes\boldsymbol{PBB}^{\mathrm{T}}\boldsymbol{P})\boldsymbol{s}(t).\end{aligned}\tag{33}$$

When the desired formation tracking is accomplished by the formation-leaders, one can get that $\lim\limits_{t\to\infty}\boldsymbol{\psi}_i(t) = \mathbf{0}$. Let $\boldsymbol{\phi}(t) = (\sqrt{\boldsymbol{G}_{\mathrm{f}}}\boldsymbol{L}_2 \otimes -\alpha_1\boldsymbol{PBB}^{\mathrm{T}}\boldsymbol{P})\boldsymbol{s}(t)$. In light of the Young's inequality, one can obtain that

$$\begin{aligned}&-2\alpha_1\boldsymbol{\varsigma}^{\mathrm{T}}(t)(\boldsymbol{G}_{\mathrm{f}}\boldsymbol{L}_2\otimes\boldsymbol{PBB}^{\mathrm{T}}\boldsymbol{P})\boldsymbol{s}(t) = \\ &\quad 2\boldsymbol{\varsigma}^{\mathrm{T}}(t)(\sqrt{\boldsymbol{G}_{\mathrm{f}}}\otimes\boldsymbol{I}_M)\boldsymbol{\phi}(t) \leqslant \\ &\quad (1-a)\boldsymbol{\varsigma}^{\mathrm{T}}(t)(\boldsymbol{G}_{\mathrm{f}}\otimes\boldsymbol{I}_M)\boldsymbol{\varsigma}(t) + \frac{1}{1-a}\|\boldsymbol{\phi}(t)\|^2,\end{aligned}\tag{34}$$

where a is a positive constant satisfying $0 < a < 1$. It follows from Eqs. (33) and (34) that

$$\begin{aligned}\dot{\boldsymbol{V}}_2(t) \leqslant &\,\boldsymbol{\varsigma}^{\mathrm{T}}(t)(\boldsymbol{G}_{\mathrm{f}}\otimes(\boldsymbol{PA}+\boldsymbol{A}^{\mathrm{T}}\boldsymbol{P}-\boldsymbol{PBB}^{\mathrm{T}}\boldsymbol{P}+ \\ &(1-a)\boldsymbol{I}_M))\boldsymbol{\varsigma}(t) + \frac{1}{1-a}\|\boldsymbol{\phi}(t)\|^2 \leqslant \\ &-a\boldsymbol{\varsigma}^{\mathrm{T}}(t)(\boldsymbol{G}_{\mathrm{f}}\otimes\boldsymbol{I}_M)\boldsymbol{\varsigma}(t) + \frac{1}{1-a}\|\boldsymbol{\phi}(t)\|^2 \leqslant \\ &-\frac{a}{\lambda_{\max}(\boldsymbol{P})}\boldsymbol{V}_2 + \frac{1}{1-a}\|\boldsymbol{\phi}(t)\|^2.\end{aligned}\tag{35}$$

Note that $\|\boldsymbol{\phi}(t)\|^2$ is bounded and a positive constant a can be designed to be arbitrarily small to ensure that $\dfrac{1}{1-a}\|\boldsymbol{\phi}(t)\|^2$ is small enough. Therefore, the Lyapunov function $\boldsymbol{V}_2(t)$ is uniformly ultimately bounded stable. And the UAV swarm system (3) can achieve the containment control under the control protocol (9) based on Definition 2.

Based on the above analyses, since $\boldsymbol{\psi}_i(t)$ is asymptotically stable and $\boldsymbol{\varsigma}_i(t)$ is ultimately bounded stable, the UAV swarm system can accomplish formation-containment tracking by using the control protocols (8) and (9) based on Definition 3. This completes the proof of the Theorem 1.

3 Numerical Simulation

A multi-UAV system with ten UAVs is considered, where the tracking-leader is denoted by $i = 0$, the formation-leaders are labeled by $i = 1, 2, \cdots, 5$, and the followers are represented by $i = 6, 7, \cdots, 9$. The formation-leaders are required to accomplish a desired time-varying formation configuration and track the state trajectory of the tracking-leader simultaneously, while the followers need to converge to the convex hull formed by the formation-leaders in the XY plane. The switching topologies of the multi-UAV system are shown in Fig. 1. This paper supposes that

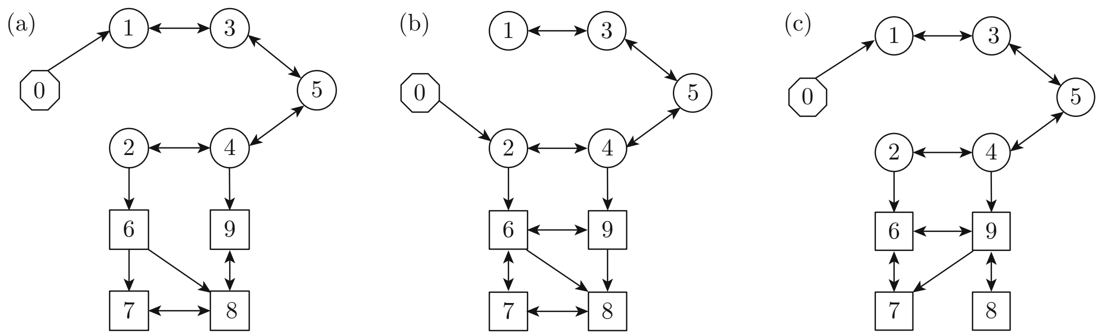

Fig. 1 Switching topologies. (a) Q1; (b) Q2; (c) Q3.

the weight of the switching topologies is 0 or 1. Additionally, the interaction topology switching signal is displayed in Fig. 2. It is aperiodic. When $\sigma(t) = 1$, the interaction topology is represented by Q1; when $\sigma(t) = 2$, the interaction topology is represented by Q2; when $\sigma(t) = 3$, the interaction topology is represented by Q3.

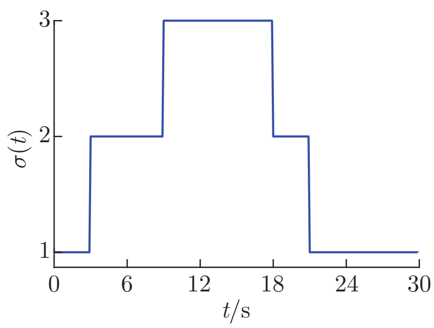

Fig. 2 Interaction topology switching signal.

The dynamics of the UAVs is denoted by (1) and (2), where $\boldsymbol{x}_i(t) = (\boldsymbol{x}_{iX}(t), \boldsymbol{x}_{iY}(t))^{\mathrm{T}}$, $\boldsymbol{v}_i(t) = (\boldsymbol{v}_{iX}(t), \boldsymbol{v}_{iY}(t))^{\mathrm{T}}$, $\boldsymbol{u}_i(t) = (\boldsymbol{u}_{iX}(t), \boldsymbol{u}_{iY}(t))^{\mathrm{T}}$, $\boldsymbol{\psi}_i(t) = (\boldsymbol{\psi}_{x_{iX}}(t), \boldsymbol{\psi}_{x_{iY}}(t), \boldsymbol{\psi}_{v_{iX}}(t), \boldsymbol{\psi}_{v_{iY}}(t))^{\mathrm{T}}$, $\boldsymbol{\varsigma}_i(t) = (\boldsymbol{\varsigma}_{x_{iX}}(t), \boldsymbol{\varsigma}_{x_{iY}}(t), \boldsymbol{\varsigma}_{v_{iX}}(t), \boldsymbol{\varsigma}_{v_{iY}}(t))^{\mathrm{T}}$ $(i = 0, 1, \cdots, 9)$. $\boldsymbol{\psi}_{x_{iX}}(t) = \boldsymbol{\xi}_{x_{iX}}(t) - \boldsymbol{h}_{x_{iX}}(t) - \boldsymbol{\xi}_{x_{0X}}(t)$, $\boldsymbol{\psi}_{x_{iY}}(t) = \boldsymbol{\xi}_{x_{iY}}(t) - \boldsymbol{h}_{x_{iY}}(t) - \boldsymbol{\xi}_{x_{0Y}}(t)$, $\boldsymbol{\psi}_{v_{iX}}(t) = \boldsymbol{\xi}_{v_{iX}}(t) - \boldsymbol{h}_{v_{iX}}(t) - \boldsymbol{\xi}_{v_{0X}}(t)$, $\boldsymbol{\psi}_{v_{iY}}(t) = \boldsymbol{\xi}_{v_{iY}}(t) - \boldsymbol{h}_{v_{iY}}(t) - \boldsymbol{\xi}_{v_{0Y}}(t)$, $\boldsymbol{\varsigma}_{x_{iX}}(t) = (\boldsymbol{L}_3 \otimes \boldsymbol{I}_n)(\boldsymbol{\xi}_{x_{iX}}(t) - (-\boldsymbol{L}_3^{-1}\boldsymbol{L}_2 \otimes \boldsymbol{I}_n)\boldsymbol{\xi}_{x_{0X}}(t))$, $\boldsymbol{\varsigma}_{x_{iY}}(t) = (\boldsymbol{L}_3 \otimes \boldsymbol{I}_n)(\boldsymbol{\xi}_{x_{iY}}(t) - (-\boldsymbol{L}_3^{-1}\boldsymbol{L}_2 \otimes \boldsymbol{I}_n)\boldsymbol{\xi}_{x_{0Y}}(t))$, $\boldsymbol{\varsigma}_{v_{iX}}(t) = (\boldsymbol{L}_3 \otimes \boldsymbol{I}_n)(\boldsymbol{\xi}_{v_{iX}}(t) - (-\boldsymbol{L}_3^{-1}\boldsymbol{L}_2 \otimes \boldsymbol{I}_n)\boldsymbol{\xi}_{v_{0X}}(t))$, $\boldsymbol{\varsigma}_{v_{iY}}(t) = (\boldsymbol{L}_3 \otimes \boldsymbol{I}_n)(\boldsymbol{\xi}_{v_{iY}}(t) - (-\boldsymbol{L}_3^{-1}\boldsymbol{L}_2 \otimes \boldsymbol{I}_n)\boldsymbol{\xi}_{v_{0Y}}(t))$. The unknown control input of the tracking-leader is described by $\boldsymbol{u}_0(t) = (1 + \cos(t), 1 + \sin(t))$, which can satisfy Assumption 3. The desired time-varying formation for the formation-leaders is as follows:

$$\boldsymbol{h}_i(t) = \begin{bmatrix} 60\cos(t + 2(i-1)\pi/5) \\ 60\sin(t + 2(i-1)\pi/5) \\ -60\sin(t + 2(i-1)\pi/5) \\ 60\cos(t + 2(i-1)\pi/5) \end{bmatrix}, \quad i = 1, 2, \cdots, 5.$$

If the desired formation $\boldsymbol{h}_i(t)$ is realized, then the trajectories of the five formation-leaders will form a regular pentagon and rotate around the tracking-leader. By solving the inequality (10), it can get positive matrix $\boldsymbol{P} = \begin{bmatrix} 1.732\,1\boldsymbol{I}_{2\times2} & \boldsymbol{I}_{2\times2} \\ \boldsymbol{I}_{2\times2} & 1.732\,1\boldsymbol{I}_{2\times2} \end{bmatrix}$. Based on Lemma 3, the positive definite matrices $\boldsymbol{D}_{\mathrm{L}}$, $\boldsymbol{\varXi}_{\mathrm{L}}$, $\boldsymbol{\varPhi}_{\mathrm{f}}$, and $\boldsymbol{G}_{\mathrm{f}}$ can be constructed, then one can obtain $\alpha_1 \geqslant 0.102\,2$ and $\alpha_2 \geqslant 2.074\,8$, so choose $\alpha_1 = 5$ and $\alpha_2 = 10$. The positive constants η and ω are set to be $\eta = 5$ and $\omega = 5$. The initial states of the tracking-leader are $\boldsymbol{x}_0(t) = (1, 1.2)^{\mathrm{T}}$, $\boldsymbol{v}_0(t) = (0, 1)^{\mathrm{T}}$. Also, the initial states of the formation-leaders are set to be $\boldsymbol{x}_1(t) = (2.0, 1.6)^{\mathrm{T}}$, $\boldsymbol{v}_1(t) = (1, 2)^{\mathrm{T}}$, $\boldsymbol{x}_2(t) = (1.3, 2.5)^{\mathrm{T}}$, $\boldsymbol{v}_2(t) = (0.5, 2.0)^{\mathrm{T}}$, $\boldsymbol{x}_3(t) = (1, 1)^{\mathrm{T}}$, $\boldsymbol{v}_3(t) = (0, 1)^{\mathrm{T}}$, $\boldsymbol{x}_4(t) = (1.5, 1.0)^{\mathrm{T}}$, $\boldsymbol{v}_4(t) = (1.0, 0.8)^{\mathrm{T}}$, $\boldsymbol{x}_5(t) = (2, 1)^{\mathrm{T}}$, $\boldsymbol{v}_5(t) = (0, 2)^{\mathrm{T}}$. The initial states of the followers are described by $\boldsymbol{x}_6(t) = (5, 0)^{\mathrm{T}}$, $\boldsymbol{v}_6(t) = (2.6, 0.8)^{\mathrm{T}}$, $\boldsymbol{x}_7(t) = (1.5, 0.5)^{\mathrm{T}}$, $\boldsymbol{v}_7(t) = (0.6, 0.6)^{\mathrm{T}}$, $\boldsymbol{x}_8(t) = (0.2, 0.5)^{\mathrm{T}}$, $\boldsymbol{v}_8(t) = (0.8, 1.6)^{\mathrm{T}}$, $\boldsymbol{x}_9(t) = (1.2, 1.5)^{\mathrm{T}}$, $\boldsymbol{v}_9(t) = (1.8, 1.6)^{\mathrm{T}}$.

The time-varying formation tracking errors $\boldsymbol{\psi}_i(t)$ and the containment errors of $\boldsymbol{\zeta}_i(t)$ in X and Y directions are given in Figs. 3 and 4, respectively. From these two figures, it can be seen that the formation tracking errors are asymptotically stable and the containment errors are uniformly ultimately bounded stable. Therefore, one can obtain that the UAV swarm system (3) can achieve the time-varying formation-containment tracking performance. The effectiveness of the control method in this paper is validated.

Figures 5 and 6 show the position and velocity snapshots of the multi-UAV systems at different instants $t = 0$, 10, 11.57, 13.14, 14.71, 16.28, 17.85, 19.43, 21, 22.57 s. As can be seen from the figure, it is periodic, and it has two cycles.

From Figs. 5 and 6, one can see that the formation-leaders realize a pentagon shape while tracking the trajectory generated by the tracking-leader. At the initial time $t = 0$, the agents are randomly distributed in the space. The formation-leaders begin to form a convex envelope after 1 s. At $t = 10$ s, the followers enter

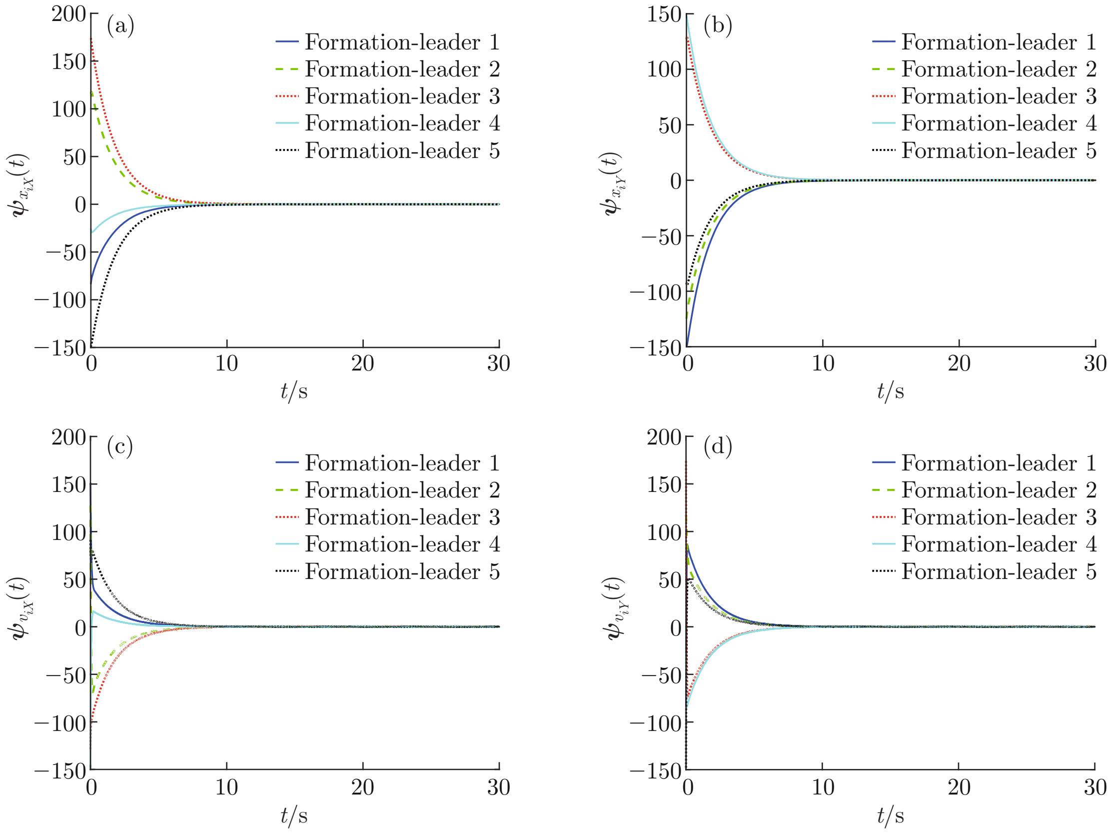

Fig. 3 Curves of the formation tracking errors. (a) Position error $\psi_{x_{iX}}$ in the X direction; (b) Position error $\psi_{x_{iY}}$ in the Y direction; (c) Velocity error $\psi_{v_{iX}}$ in the X direction; (d) Velocity error $\psi_{v_{iY}}$ in the Y direction.

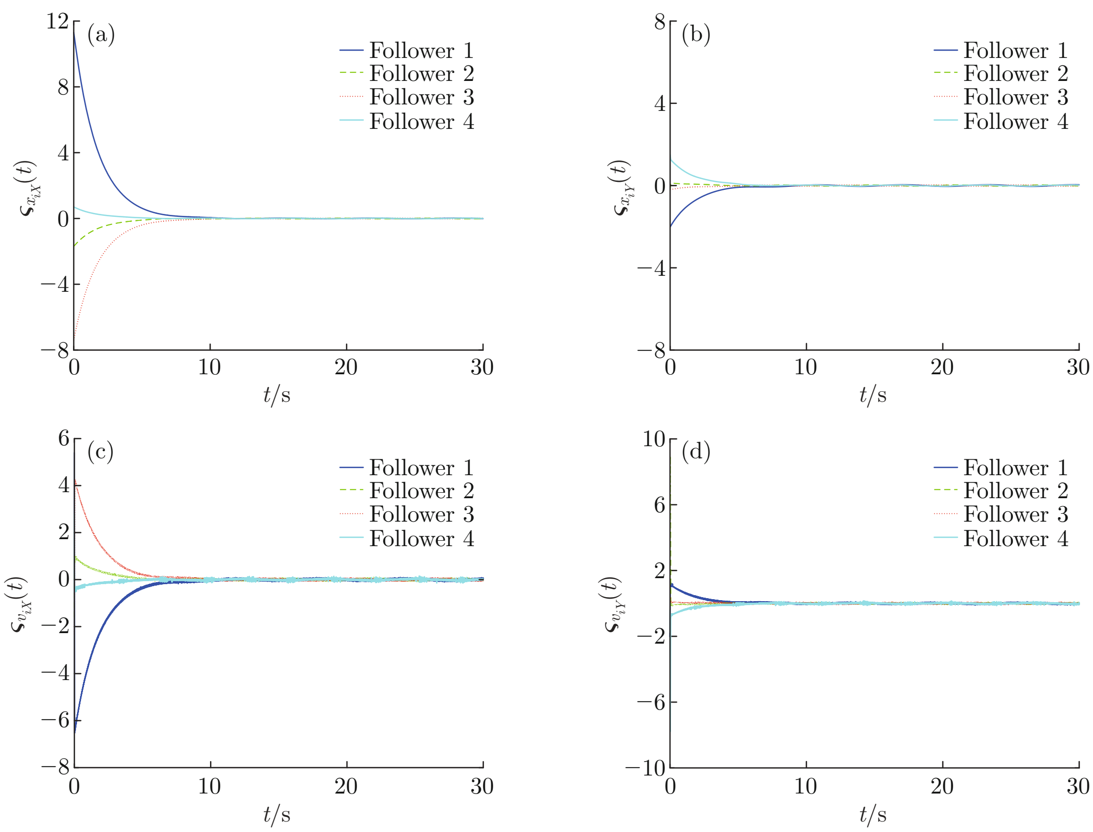

Fig. 4 Curves of the containment errors. (a) Position error $\varsigma_{x_{iX}}$ in the X direction; (b) Position error $\varsigma_{x_{iY}}$ in the Y direction; (c) Velocity error $\varsigma_{v_{iX}}$ in the X direction; (d) Velocity error $\varsigma_{v_{iY}}$ in the Y direction.

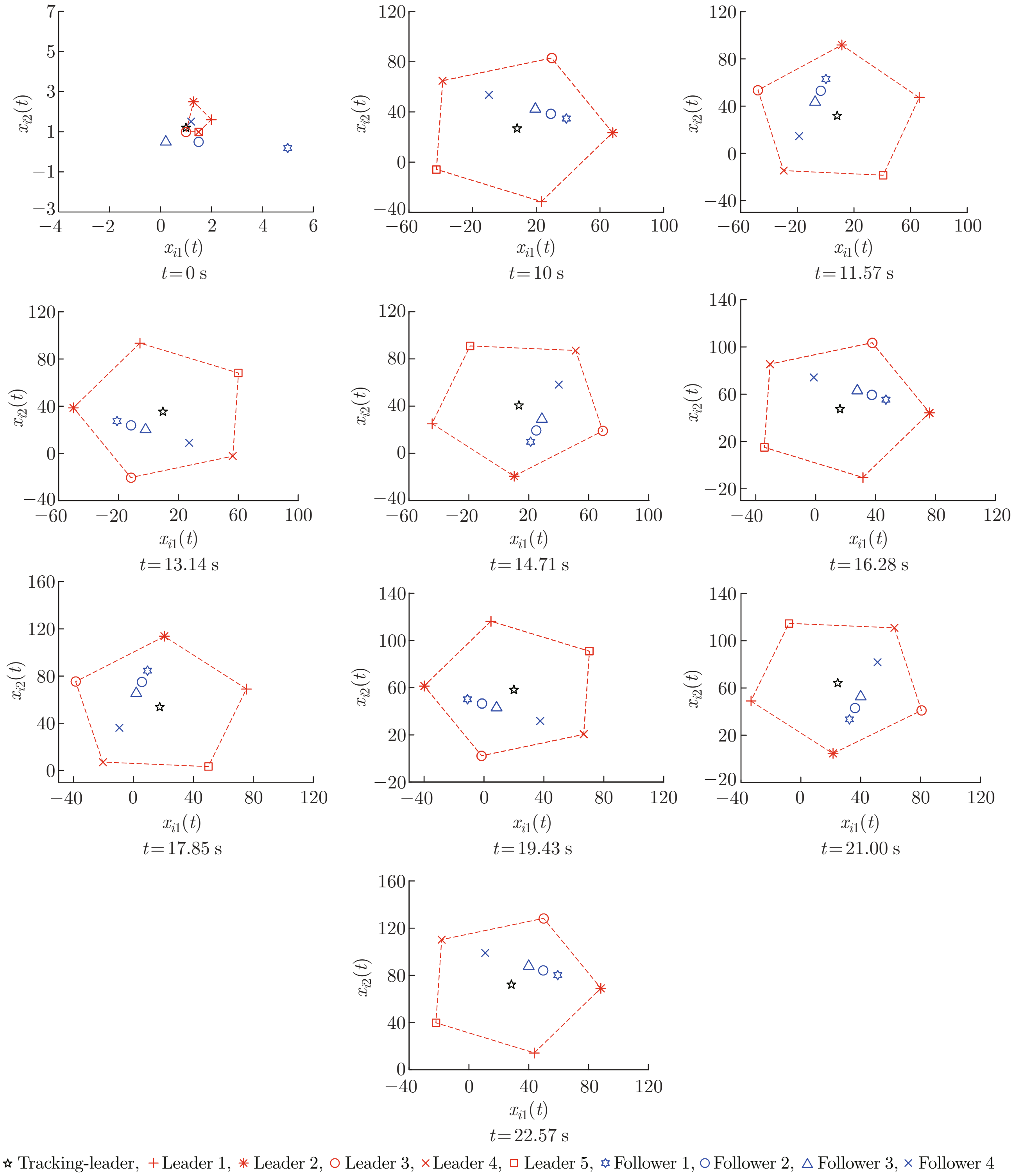

Fig. 5 Position snapshots for the UAVs.

into the convex envelope generated by the formation-leaders. Different snapshots at $t = 11.57$, 13.14, 16.28, 17.85, 19.43, 21, 22.57 s show that the formation-leaders have formed a pentagon shape, the center of which is the tracking-leader, and the followers maintain in the pentagon spanned by the formation-leaders. One can also see that the formation-leaders rotate around the tracking-leader, which implies that the achieved formation is time-varying. Since the formation tracking error tends to zero in finite time, the accomplished formation

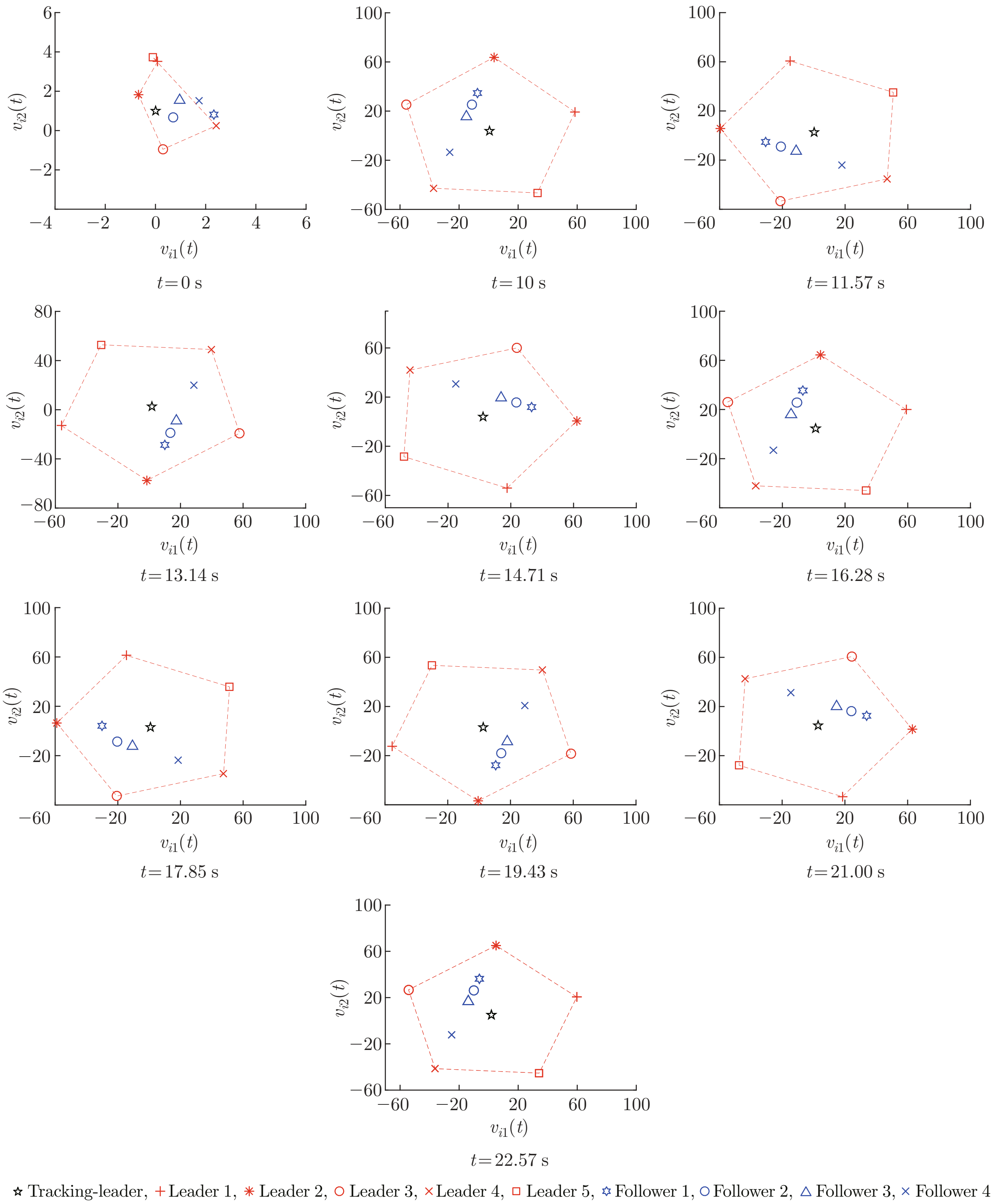

Fig. 6 Velocity snapshots for the UAVs.

configuration is the predefined formation shape. Therefore, under the protocols (8) and (9), the multi-UAV systems can realize finite-time formation-containment tracking.

4 Conclusion

The time-varying formation-containment tracking problem for multi-UAV systems with switching topologies and unknown control input is investigated. Based on the consensus control theory, the designed control protocol only depends on the part of the information of neighboring UAVs. Moreover, the limitation of knowing the boundary information of the tracking-leader's control input is removed and the high gain is avoided. Based on the Lyapunov stability theory, the stability of the multi-UAV systems and the effectiveness of the control protocol are proved. The formation-leaders can accomplish the desired time-varying formation and track the trajectory of the tracking-leader, and the states of followers can converge to the convex hull spanned by those of the formation-leaders. An interesting topic for future research is to deal with the fault-tolerant time-varying formation-containment tracking control problems for multi-UAV systems with switching topologies and actuator faults.

Conflict of Interest The authors declare that they have no conflict of interest.

References

[1] HE W, ZHANG S. Control design for nonlinear flexible wings of a robotic aircraft [J]. *IEEE Transactions on Control Systems Technology*, 2017, **25**(1): 351-357.

[2] HAN J L, CHEN Y Q. Multiple UAV formations for cooperative source seeking and contour mapping of a radiative signal field [J]. *Journal of Intelligent & Robotic Systems*, 2014, **74**(1): 323-332.

[3] WILLIAMSON W R, ABDEL-HAFEZ M F, RHEE I, et al. An instrumentation system applied to formation flight [J]. *IEEE Transactions on Control Systems Technology*, 2007, **15**(1): 75-85.

[4] MAZA I, KONDAK K, BERNARD M, et al. Multi-UAV cooperation and control for load transportation and deployment [J]. *Journal of Intelligent and Robotic Systems*, 2010, **57**(1): 417-449.

[5] SUH J, YOU S, CHOI S, et al. Vision-based coordinated localization for mobile sensor networks [J]. *IEEE Transactions on Automation Science and Engineering*, 2016, **13**(2): 611-620.

[6] YUN B, CHEN B M, LUM K Y, et al. Design and implementation of a leader-follower cooperative control system for unmanned helicopters [J]. *Journal of Control Theory and Applications*, 2010, **8**(1): 61-68.

[7] LI N H M, LIU H H T. Formation UAV flight control using virtual structure and motion synchronization [C]//*2008 American Control Conference*. Seattle: IEEE, 2008: 1782-1787.

[8] QIU H X, DUAN H B, FAN Y M. Multiple unmanned aerial vehicle autonomous formation based on the behavior mechanism in pigeon flocks [J]. *Control Theory & Applications*, 2015, **32**(10): 1298-1304 (in Chinese).

[9] KURIKI Y, NAMERIKAWA T. Consensus-based cooperative formation control with collision avoidance for a multi-UAV system [C]//*2014 American Control Conference*. Portland: IEEE, 2014: 2077-2082.

[10] WANG P, ZHANG Z F, CAO M C, et al. Research status and development of multi-UAVs formation based on consensus [J]. *Ship Electronic Engineering*, 2017, **37**(9): 1-9 (in Chinese).

[11] ABDESSAMEUD A, TAYEBI A. Formation control of VTOL Unmanned Aerial Vehicles with communication delays [J]. *Automatica*, 2011, **47**(11): 2383-2394.

[12] WANG D D, ZONG Q, ZHANG B Y. Distributed adaptive finite-time formation control of multiple UAV helicopter system [C]//*2018 37th Chinese Control Conference*. Wuhan: IEEE, 2018: 2631-2636.

[13] HUA Y Z, DONG X W, LI Q D, et al. Fault-tolerant time-varying formation control for second-order multi-agent systems with directed topologies [C]//*2017 13th IEEE International Conference on Control & Automation*. Ohrid: IEEE, 2017: 467-472.

[14] ZHENG Y S, ZHAO Q, MA J Y, et al. Second-order consensus of hybrid multi-agent systems [J]. *Systems & Control Letters*, 2019, **125**: 51-58.

[15] HOSSEINZADEH YAMCHI M, MAHBOOBI ESFANJANI R. Distributed predictive formation control of networked mobile robots subject to communication delay [J]. *Robotics and Autonomous Systems*, 2017, **91**: 194-207.

[16] JI X K, HAI J T, LUO W G, et al. Obstacle avoidance in multi-agent formation process based on deep reinforcement learning [J]. *Journal of Shanghai Jiao Tong University* (*Science*), 2021, **26**(5): 680-685.

[17] WANG J, SHI L R. Semi-global consensus problems of discrete-time multi-agent systems in the presence of input constraints [J]. *Journal of Shanghai Jiao Tong University* (*Science*), 2020, **25**(3): 288-298.

[18] WANG P, JIA Y M. Distributed containment control of second-order multi-agent systems with inherent nonlinear dynamics [J]. *IET Control Theory & Applications*, 2014, **8**(4): 277-287.

[19] LI T, LI Z P, FEI S M, et al. Second-order event-triggered adaptive containment control for a class of multi-agent systems [J]. *ISA Transactions*, 2020, **96**: 132-142.

[20] LI Z K, REN W, LIU X D, et al. Distributed containment control of multi-agent systems with general linear dynamics in the presence of multiple leaders [J]. *International Journal of Robust and Nonlinear Control*, 2013, **23**(5): 534-547.

[21] LI P Y, JABBARI F, SUN X M. Containment control of multi-agent systems with input saturation and unknown leader inputs [J]. *Automatica*, 2021, **130**: 109677.

[22] WANG Y Q, WU Q H, WANG Y. Containment control for multiple quadrotors with stationary leaders under directed graphs [C]//*2012 IEEE 51st IEEE Conference on Decision and Control*. Maui: IEEE, 2012: 2781-2786.

[23] DONG X W, HUA Y Z, ZHOU Y, et al. Theory and experiment on formation-containment control of multiple multirotor unmanned aerial vehicle systems [J]. *IEEE Transactions on Automation Science and Engineering*, 2019, **16**(1): 229-240.

[24] CHEN L M, LI C J, GUO Y N, et al. Formation-containment control of multi-agent systems with communication delays [J]. *ISA Transactions*, 2022, **128**(Pt A): 32-43.

[25] DONG X W, SHI Z Y, LU G, et al. Formation-containment analysis and design for high-order linear time-invariant swarm systems [J]. *International Journal of Robust and Nonlinear Control*, 2015, **25**(17): 3439-3456.

[26] ZHANG J X, SU H S. Formation-containment control for multi-agent systems with sampled data and time delays [J]. *Neurocomputing*, 2021, **424**: 125-131.

[27] GAO Z Y, ZHANG H G, WANG Y C, et al. Time-varying output formation-containment control for homogeneous/heterogeneous descriptor fractional-order multi-agent systems [J]. *Information Sciences*, 2021, **567**: 146-166.

[28] CAI Y L, ZHANG H G, WANG Y C, et al. Adaptive bipartite fixed-time time-varying output formation-containment tracking of heterogeneous linear multiagent systems [J]. *IEEE Transactions on Neural Networks and Learning Systems*, 2022, **33**(9): 4688-4698.

[29] XU B, WANG Z Y, LI W H, et al. Distributed robust model predictive control-based formation-containment tracking control for autonomous underwater vehicles [J]. *Ocean Engineering*, 2023, **283**: 115210.

[30] HUA Y Z, DONG X W, HAN L, et al. Formation-containment tracking for general linear multi-agent systems with a tracking-leader of unknown control input [J]. *Systems & Control Letters*, 2018, **122**: 67-76.

[31] LIAO R W, HAN L, DONG X W, et al. Finite-time formation-containment tracking for second-order multi-agent systems with a virtual leader of fully unknown input [J]. *Neurocomputing*, 2020, **415**: 234-246.

[32] LU Y Z, DONG X W, LI Q D, et al. Time-varying group formation-containment tracking control for general linear multiagent systems with unknown inputs [J]. *IEEE Transactions on Cybernetics*, 2022, **52**(10): 11055-11067.

[33] ZHANG X Y, WU J, ZHAN X S, et al. Observer-based adaptive time-varying formation-containment tracking for multiagent system with bounded unknown input [J]. *IEEE Transactions on Systems, Man, and Cybernetics: Systems*, 2023, **53**(3): 1479-1491.

[34] CHEN L J, HAN T, XIAO B, et al. Predefined-time hierarchical controller-estimator time-varying formation-containment tracking for multiple Euler-Lagrange systems with two-layer leaders [J]. *Journal of the Franklin Institute*, 2023, **360**(7): 5242-5266.

[35] WEI Z Q, WENG Z M, HUA Y Z, et al. Formation-containment tracking control for heterogeneous unmanned swarm systems with switching topologies [J]. *Acta Aeronautica ET Astronautica Sinica*, 2021, **44**(2): 252-267 (in Chinese).

[36] NI W, CHENG D Z. Leader-following consensus of multi-agent systems under fixed and switching topologies [J]. *Systems & Control Letters*, 2010, **59**(3/4): 209-217.

[37] ZHENG R H, LIU Y H, SUN D. Enclosing a target by nonholonomic mobile robots with bearing-only measurements [J]. *Automatica*, 2015, **53**: 400-407.